

## Effect of grain size on deformation-induced martensite formation in 304 and 316 stainless steels during room temperature tensile testing

S. K. VARMA, J. KALYANAM, L. E. MURR, V. SRINIVAS

Department of Metallurgical and Materials Engineering, The University of Texas at El Paso, El Paso, Texas 79968-0520 USA

The stability of austenite in 304 and 316 stainless steels (SS) is one of the important characteristics for their various practical applications, including corrosion resistance and work hardening capabilities. If it is assumed that the presence of martensite along with austenite can decrease the corrosion resistance then the formation of martensite, deformation-induced martensite (DIM), should certainly be undesirable in SS. However, forming operations may be such that the resistance to the formation of DIM may not be controllable. Thus, factors influencing DIM formation must be carefully studied, and methods should be developed to circumvent their formation, at least in the final product.

There are two types of deformation-induced martensites formed in ferrous systems: stress-assisted martensite (SAM) and strain-induced martensite (SIM). SAM is formed by the applied stress in a manner similar to the nucleation and growth of conventional thermal martensite [1, 2]. Even though morphologically SAM has been observed mainly in plate form, the observation of laths is also quite common. The magnitude of plastic deformation determines the formation of SIM and consists of only lath type morphology.

The mechanisms proposed for the formation of DIM (only SIM will be considered in this paper) can be divided into two basic steps: (i) nucleation and (ii) growth [3-16]. The mechanism for the nucleation of DIM in  $\alpha'$  form was first introduced by Olsen and Cohen [3-6]. They proposed that specific, invariant, atomic displacements for nucleation takes place on intersecting  $\{111\}$  planes in the austenite phase. More recent studies by Hecker *et al.* [9] and Murr *et al.* [10] have shown that TEM studies clearly indicate that microshear band intersections within a grain are the most preferred sites for the nucleation process during the deformation of 304 SS during uniaxial and multiaxial types of deformation. The growth of DIM nuclei does not take place by means of conventional growth of precipitates but a process of coalescence of some of the nearby nuclei results in the increase in size of the  $\alpha'$  DIM.

The experimental variables which have been

investigated to study the kinetics of DIM formation are the amount of strain, strain state, strain rate and deformation temperature. The present study deals with the effect of austenite grain size on the characteristics of DIM formed during room temperature tensile testing in 304 SS. The amount of DIM at corresponding true strains has been related to grain sizes and flow stresses in tension. A 316 SS was used to compare the results with 304 SS under identical conditions of deformation because 316 SS is generally not considered as a martensite former.

The 304 SS was purchased in the form of a plate with dimensions of 122(l), 91(w) and 0.635(t) cm. The tensile samples were fabricated from this plate with lengths and widths reduced to 10.16 and 1.27 cm, respectively. The 316 SS samples were also fabricated with identical dimensions. The chemical compositions of the two stainless steels in weight per cent are shown in Table I. It must be noted from this table that the only difference in the compositions of the two stainless steels used in this study is in the weight per cent of nickel (13.48% in 316 and 8.19% in 304 stainless steel) and molybdenum (2.34% in 316 and 0.27% in 304 stainless steel). Isochronal annealing for 1 h at temperatures in the range 900-1300 °C yielded grain sizes of 53-285  $\mu\text{m}$ , respectively, in 304 SS. The grain sizes of 125 and 200  $\mu\text{m}$  were obtained in 316 SS by isothermal annealing at 1175 °C for 1 and 3 h, respectively. The details of the heat treatments in the two stainless steels are given in Table II. It was observed that the solution treatment of these alloys resulted in the formation of martensite, as indicated by instru-

TABLE II Heat treatment schedules for 304 and 316 stainless steels

Material	Temperature (°C)	Time (h)	Grain size ( $\mu\text{m}$ )
304	900	1	53
	1050	1	123
	1100	1	180
	1300	1	285
316	1175	1	125
	1175	3	200

TABLE I Chemical compositions of 304 and 316 stainless steels by weight per cent

Material	C	Mn	P	S	Si	Ni	Cr	Mo	Co	Cu
304	0.054	1.730	0.034	0.014	0.350	8.19	18.33	0.270	0.120	0.250
316	0.057	1.860	0.024	0.019	0.580	13.48	17.25	2.340	0.020	0.100

mental magnetic measurements after the quenching operation.

The martensite formed from austenite is ferromagnetic and can be detected by magnetic permeability measurements, which were made in this study with a Ferritescope (Model # Autofest-Fe). The instrument was calibrated with standard iron samples. A small magnetic field is applied to the sample with the help of a two-point probe placed on the sample, and the output in the form of a voltage is an indication of the amount of permeability, which is directly proportional to the amount of martensite in the sample since the austenite is non-magnetic. The instrument simply gives the ferrite number of the specimen which can be converted into volume fraction martensite ( $\alpha'$ ) with the help of standard calibration curves.

The tensile samples used in this study did not have a reduced gauge section in them and were tested in an INSTRON-1127. The ratio of the crosshead speed to the gauge length gives the strain rate and the three different strain rates used in this study were 5, 0.5 and 0.01/min. Samples of a particular grain size were tested at a given strain rate by deforming to 10, 30, 40 and 50% engineering strain values and then the loads were removed for  $\alpha'$  measurements. The tests were then repeated for each grain size and strain rate mentioned above.

Standard techniques of mechanical polishing were employed to prepare the samples for optical microscopy needed for the measurements of grain sizes. The electroetching was carried out in an electrolyte of 60% by volume, nitric acid solution at a 10 V DC voltage using a stainless steel anode. The grain sizes were calculated using the linear intercept method and the mean intercept length (obtained by counting at least 500 grain boundary intersections with the test line) was multiplied by the shape factor 1.68 to obtain grain diameters.

Fig. 1 shows the effect of strain rate on the flow stress versus percentage engineering strain behaviour for 304 SS during room temperature tensile testing for four different grain sizes. Three different

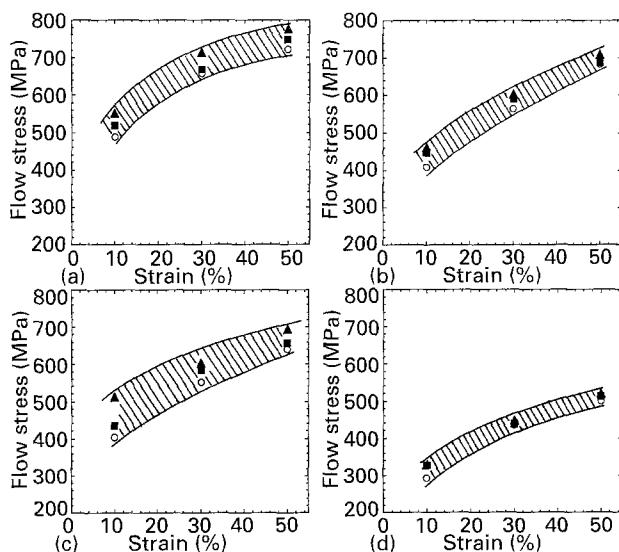


Figure 1 The effect of strain on the flow stress versus percentage strain curves at three strain rates and four grain sizes: (a) 53, (b) 123, (c) 180 and (d) 285  $\mu\text{m}$  ( $\circ$  0.01/min;  $\blacksquare$  0.5/min;  $\blacktriangle$  5/min).

strain rates have been used for each grain size of 304 SS in Fig. 1. It must be noted that this figure does not represent the normal tensile stress-strain curve of stainless steel. A sample of steel with a grain size of 53  $\mu\text{m}$  was pulled in tension at a strain rate of 0.01/min to an engineering strain of 10% and the flow stress was recorded. Similarly other samples of identical grain size were deformed to 30 and 40% engineering strain at the same rate, and the flow stresses were recorded. The complete procedure was repeated for the other three grain sizes (123, 180 and 285  $\mu\text{m}$ ) at two more strain rates (0.5 and 5/min).

The effect of strain rate on the flow stress values appears to follow the well-established relationship between the two, where the flow stress increases with increase in strain rate at a given value of percentage strain and grain size. However, Fig. 1 also shows that the differences between the flow stress values at a constant engineering strain for different grain sizes decrease as the grain size increases except in the case of 180  $\mu\text{m}$ . The effect can be easily recognized by inspection of the cross-hatched areas in the four graphs of this figure. This would, perhaps, indicate strain rate insensitivity towards the flow stress values at larger grain sizes. One of the ways in which the observation may be tested for its complete validity would be to examine the strain rate sensitivity in the single crystal form. This strain rate insensitivity at larger grain sizes has also been observed in copper [22], aluminium [23] and nickel [24].

Fig. 2 shows a comparison of the flow stress values of 304 SS at different percentage engineering strains with 316 SS for similar grain sizes at a strain rate of 0.5/min. The grain size effect is quite evident in both cases and grain size dependence is also similarly exhibited by the two curves in each graph of Fig. 2. The widths of the 'bands' shown in this figure also decreases with an increase in grain size at a given strain rate of deformation. According to Ashby's model [25, 26] the deformation of polycrystalline

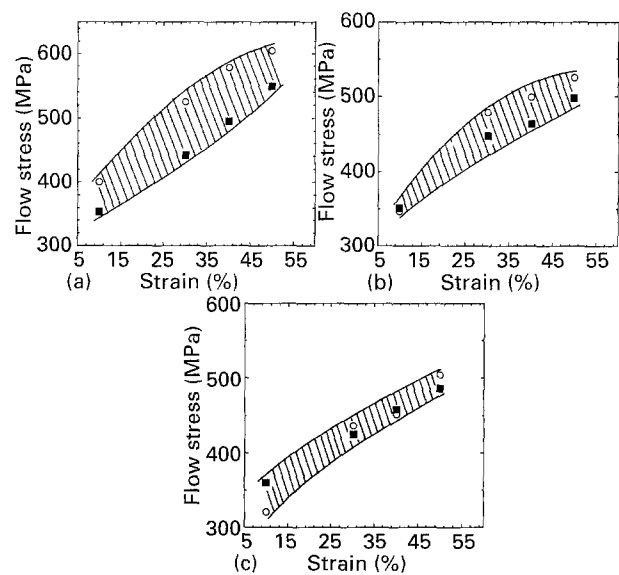


Figure 2 Comparative analysis of flow stress profile against percentage strain for almost similar grain sizes in 304 and 316 SS: (a)  $\circ$  304-53  $\mu\text{m}$ ;  $\blacksquare$  316-75  $\mu\text{m}$ ; (b)  $\circ$  304-123  $\mu\text{m}$ ,  $\blacksquare$  316-125  $\mu\text{m}$ ; (c)  $\circ$  304-180  $\mu\text{m}$ ,  $\blacksquare$  316-200  $\mu\text{m}$ .

metals during tensile testing may be divided into two major components: deformation controlled by the (a) geometrically necessary dislocations (GNDs) and (b) statistically stored dislocations (SSDs). It is expected that the contributions from the GNDs would be dominating in the beginning of the deformation while the latter part of the deformation may be primarily due to SSDs. Thus as the engineering strain increases during the deformation the effect of grain size becomes negligible and other dislocation interactions, such as chance encounters of the dislocations (from both long-range as well as short-range interactions), characteristics of SSDs, control the deformation. Since the contributions from the SSDs is not related to the grain size, the differences between the flow stress values at the start of the deformation and towards the end is expected to be more pronounced at smaller grain sizes and this discussion appears to be in agreement with the experimental observations shown in Fig. 2. The experimental data in tension on 304 SS by Murr and Wang [27] shows a continuous increase in dislocation density near the grain boundaries, as well as in the grain interior, as the strain increases, but the value of dislocation density in the grain interior was found to be higher than at the areas adjacent to grain boundaries only at higher tensile strain values. Thus the behaviour shown in Fig. 2 and our explanation appears to be reasonable.

The Hall-Petch plots (graph between flow stress  $\sigma$  and inverse square root of the grain diameter  $D^{-1/2}$  according to the equation,  $\sigma = \sigma_0 + K(D)^{-1/2}$ , where  $\sigma_0$  and  $K$  are materials constants) were made and Fig. 3 shows the changes in the slope values ( $K$ ) as a function of percentage strain for the two SS. The graph may actually be interpreted in two different ways: (a) A linear relationship between the two parameters may be assumed. A least square fit line can be drawn through the data points even though considerable scatter in the data for 304 SS will be present. The lines appear to have similar slope in 304 SS and 316 SS but 304 SS shows higher  $K$  values for the entire range of strain values of this study. The differences may be explained on the basis of the

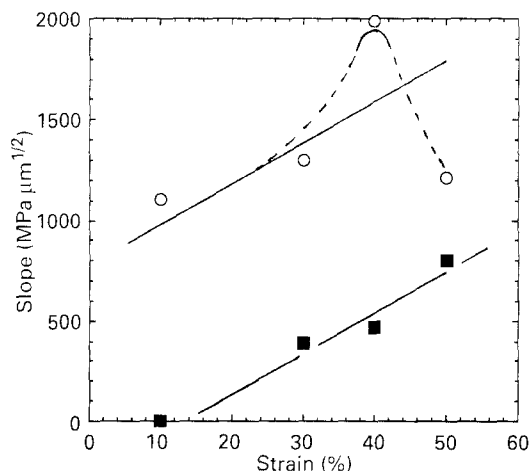


Figure 3 The variation in the values of the slopes of the Hall-Petch plots with percentage strain in 304 and 316 SS (○ 304; ■ 316).

formation of measurable DIM in 304 SS and a general absence of DIM in 316 SS. This would indicate that the Hall-Petch equation is capable of simply absorbing the additional strengthening due to DIM. (b) The data points are simply interpolated which results in a monotonic increase in  $K$  values for 316 SS up to a maximum tensile strain of 50%. The 304 SS shows an increase in  $K$  values up to 40% engineering strain and then decreases to a 50% strain in tension. If the  $K$  value is considered to be the strengthening effectiveness due to both grain size and DIM, then as the percentage strain increases during room temperature tensile testing the contributions from GNDs (in this case contributions from both grain boundaries and DIM will have to be taken into consideration) should decrease, which can explain the lower  $K$  value at 50% strain shown in Fig. 4. Once again, the comparison between the two curves will involve the important consideration that DIM was only found to form in 304 SS, as will be discussed in the next paragraph.

Fig. 4 shows the variation of the amount of DIM formed as a function of strain during the uniaxial tensile testing of 304 and 316 SS for three different grain diameters. It can be seen that the volume fraction of DIM increases with increase in strain in

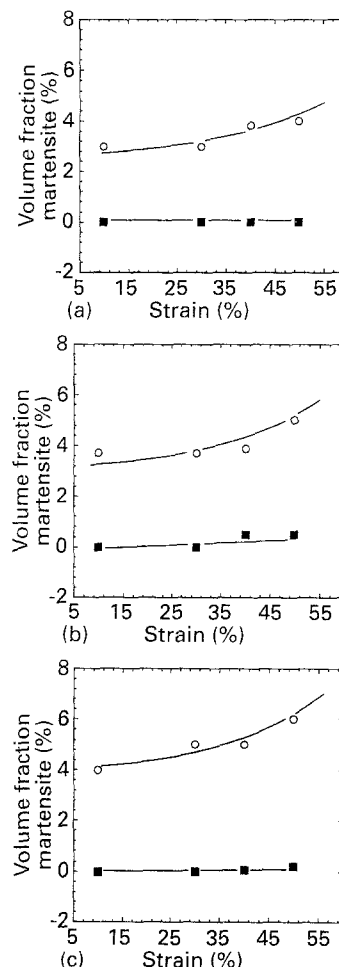


Figure 4 Comparative analysis of the percentage volume fraction of martensite formed against percentage strain for almost similar grain sizes of 304 and 316 SS. The graph has been extended on the percentage martensite axis towards the negative side for the sake of convenience only since most of the data points are very close (but positive) to zero value: (a) ○ 304-53  $\mu\text{m}$ , ■ 316-75  $\mu\text{m}$ ; (b) ○ 304-123  $\mu\text{m}$ , ■ 316-125  $\mu\text{m}$ ; (c) ○ 304-180  $\mu\text{m}$ , ■ 316-200  $\mu\text{m}$ .

304 SS while there is no appreciable change in the value for the volume fraction of DIM in 316 SS up to a maximum tensile strain of 50%. The ordinates on the graph in Fig. 4 (also in Fig. 6) have been drawn to negative values only because the data points are so close to zero per cent that they would all fall on the percentage strain axis otherwise. Obviously, negative values of per cent martensite have no meaning. It was also observed that there was no change in the amount of DIM formed in both SS at different values of strain rates.

Murr *et al.* [10] have shown that the change in deformation mode from uniaxial to multiaxial increases the amount of DIM in 304 stainless steel (with a grain size of 15  $\mu\text{m}$ ). In order to investigate the effect of strain state and grain size on the formation of DIM in both 304 and 316 stainless steels, the amount of DIM formed during room temperature rolling was measured. Fig. 5 shows the results of such an experiment and the data for the tensile testing have been included in the graphs. It can be seen from this figure that the amount of DIM formed may extend from 5 to 45% during rolling reduction of 304 stainless steel with a grain diameter of 285  $\mu\text{m}$  while a maximum of 30% change in the amount of DIM was observed for the 53  $\mu\text{m}$  grain diameter case. This shows that the amount of DIM formed is quite sensitive to the grain size in 304 stainless steel especially during rolling, as well as during tensile testing.

Even though no change in the DIM formation was observed in 316 stainless steel during room temperature tensile testing, rolling experiments indicate a significant amount of DIM formation. Fig. 6 compares the amounts of DIM formed during the room temperature tensile testing and rolling at various true strain values. It must be noted that it is generally believed that no DIM is formed in 316 stainless steels. However, the results of this study clearly demonstrate the presence of  $\alpha'$  in this SS.

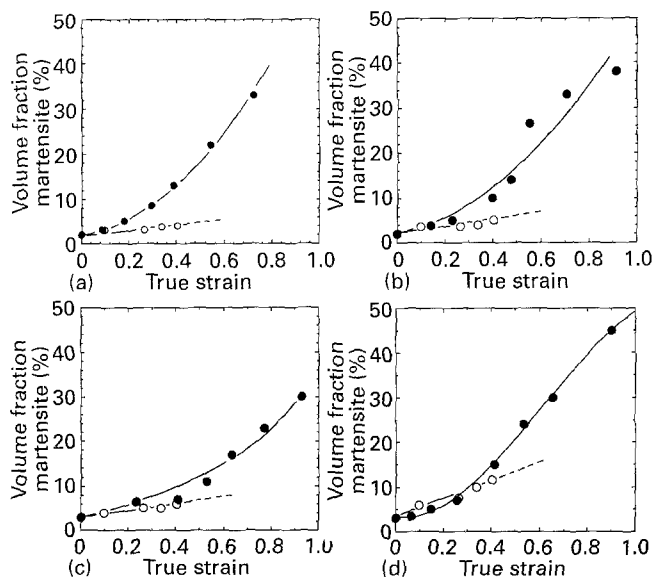


Figure 5 Comparative analysis of percentage volume fraction of martensite against true strain in rolling and uniaxial tension in 304 SS for grain sizes of (a) 53, (b) 123, (c) 180 and (d) 285  $\mu\text{m}$  (○ 304 uniaxial tension, ● 304 rolled).

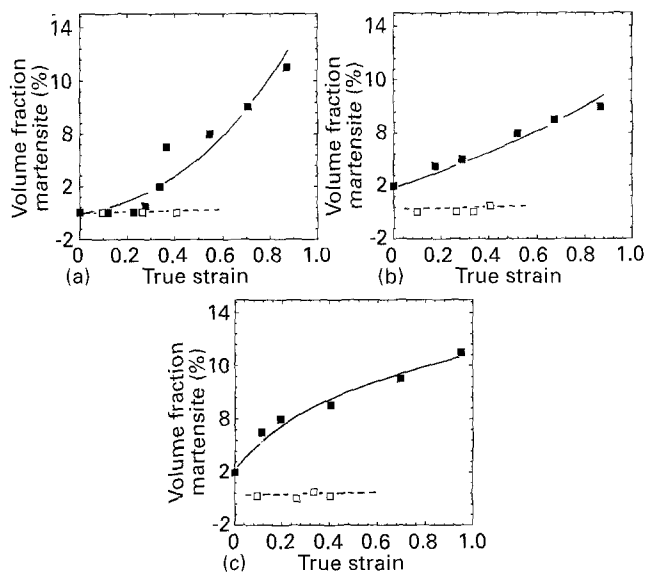


Figure 6 Comparative analysis of percentage volume fraction martensite against true strain in rolling and uniaxial tension in 316 SS for grain sizes of (a) 75, (b) 125 and (c) 200  $\mu\text{m}$ . The graph has been extended on the percentage martensite axis towards the negative side for the sake of convenience only since most of the data points are very close (but positive) to zero value (□ 316 uniaxial tension, ■ 316 rolled).

Furthermore, the formation of  $\alpha'$  martensite in 316 SS is strain state dependent. The grain size dependence on the DIM formation is also exhibited by 316 stainless steel but the magnitude of this dependence is much smaller in comparison to 304 stainless steel.

A study of the comparison of the deformation behavior of 304 and 316 SS presented in this paper shows some of the following significant features: (1) Similar grain size strengthening has been confirmed in 304 and 316 SS during room temperature tensile testing. (2) The slope of the Hall-Petch plots have been shown to be affected by the formation of DIM in 304 SS. (3) The 316 SS does not form DIM under the conditions of tensile testing used in this study. (4) The DIM formation, however, does take place in 316 SS when the deformation mode is changed from room temperature tensile testing to rolling. (5) The extent of DIM formed in both rolling and tensile testing is much higher in 304 SS compared to 316 SS. (6) The DIM formation appears to be grain size sensitive in both 304 and 316 SS.

## Acknowledgements

This work was supported, in part, by a Murchison endowment at The University of Texas at El Paso. We are grateful to Dr K. P. Staudhammer for making a commercial Ferritescope available for this work.

## References

1. P. C. MAXWELL, A. GOLDBERG and J. C. SHYNE, *Metall. Trans.* **5** (1974) 1305.
2. J. R. PATEL and M. COHEN, *Acta Metall.* **1** (1953) 531.
3. G. B. OLSEN and M. COHEN, *Metall. Trans. A* **6A** (1975) 791.
4. *Idem., ibid.* **7A** (1976) 1897.
5. *Idem., ibid.* **7A** (1976) 1905.
6. *Idem., ibid.* **7A** (1976) 1915.

7. G. B. OLSEN and M. AZRIN, *ibid.* **8A** (1978) 713.
8. K. P. STAUDHAMMER, C. E. FRANTZ, S. S. HECKER and L. E. MURR, in "Shock waves and high-strain-rate phenomenon in metals", edited by M. A. Meyers and L. E. Murr (Plenum, New York, 1981) p. 91.
9. S. S. HECKER, M. G. STOUT, K. P. STAUDHAMMER and J. L. SMITH, *Metall. Trans. A* **13A** (1982) 619.
10. L. E. MURR, K. P. STAUDHAMMER and S. S. HECKER, *ibid.* **13A** (1982) 627.
11. L. E. MURR and K. P. STAUDHAMMER, *Scripta Metall.* **16** (1982) 713.
12. K. P. STAUDHAMMER, L. E. MURR and S. S. HECKER, *Acta Metall.* **31** (1983) 267.
13. *Idem.*, in Proceedings of International Conference on Solid State Transformations, edited by H. I. Aaronson (Carnegie-Mellon University, Pittsburgh, PA, 1981) p. 1287.
14. L. E. MURR, A. ADVANI, S. SHANKAR and D. G. ATTERIDGE, *Mater. Characterization* **24** (1990) 135.
15. X. F. FANG and W. DAHL, *Mater. Sci. Eng.* **A141** (1991) 189.
16. T. SUZUKI, H. KOJIMA, K. SUZUKI, T. HASHI-MOTO and M. ICHIHARA, *Acta Metall.* **25** (1977) 1151.
17. R. LAGNEBORG, *Acta Metall.* **12** (1964) 823.
18. F. LECROISEY and A. PINEAU, *Metall. Trans.* **3** (1971) 387.
19. J. DASH and H. M. OTTE, *Acta Metall.* **11** (1963) 1169.
20. J. W. BROOKS, M. H. LORETTO and R. E. SMALLMAN, *Acta Metall.* **27** (1979) 1829.
21. *Idem.*, *ibid.* **27** (1979) 1847.
22. H. SHANKARANARAYAN, Unpublished work, M.S. Thesis, The University of Texas at El Paso (May 1993).
23. DEEPAK SIL and S. K. VARMA, *Metall. Trans.* **24A** (1993) 1153.
24. JYOTHI G. RAO and S. K. VARMA, *ibid.* in press.
25. M. F. ASHBY, *Phil. Mag.* **21** (1970) 399.
26. A. W. THOMPSON, M. I. BASKES and W. F. FLANAGAN, *Acta Metall.* **21** (1973) 1017.
27. L. E. MURR and S.-H. WANG, *Res. Mechanica* **4** (1982) 237.

*Received 26 July  
and accepted 1 September 1993*